Journal of Robotics and Control (JRC)
Volume 5, Issue 2, 2024
ISSN: 2715-5072, DOI: 10.18196/jrc.v5i2.20581

Power Management and Voltage Regulation in DC Microgrid with Solar Panels and Battery Storage System

Ashraf Abdualateef Mutlag [1], Mohammed Kdair Abd [2], Salam Waley Shneen [3*]
[1, 2] Electrical Engineering Department, University of Technology, Iraq
[3] Energy and Renewable Energies Technology Center, University of Technology, Iraq
Email: [1] eee.21.10@grad.uotechnology.edu.iq, [2] mohammed.k.abd@uotechnology.edu.iq,
[3] salam.w.shneen@uotechnology.edu.iq
*Corresponding Author

***Abstract*—Photovoltaics are one of the most important renewable energy sources to meet the increasing demand for energy. This led to the emergence of Microgrid s, which revealed a number of problems, the most important of which is managing and monitoring their operation, this research contributes mainly by using a maximum power tracking algorithm Which depends on artificial neurons and integrating it with a proposed algorithm for energy management in Standalone DC Microgrid, in order to control the distribution of power and maintain the DC bus voltage level. Maximum Power Point Tracking (MPPT) algorithm based on ANN+PID is used. Where ANN tracks the maximum power point by estimating the reference voltage using real-time data such as temperature and solar radiation. The PI controller reduces the error between the measured voltage and the reference voltage and makes the necessary adjustments in order to control the boost converter connected to the photovoltaic panels. While the process of controlling the DC bus voltage level is done by controlling the battery charging and discharging process through the power management algorithm and controlling the Bidirectional converter switches according to the battery's state of charge. The simulation results obtained by used MATLAB Simulink are shown that the used MPPT algorithm achieved the maximum power with the least amount of fluctuation, the method's efficiency was 99.92%, and its accuracy was 99.85%, as well as the success of the power management algorithm controlling the battery charging/discharging process and maintaining the DC voltage level at the specified value in different operating scenarios.**

Keywords—DC Microgrid; Photovoltaic (PV) Systems; Maximum Power Point Tracking (MPPT); Voltage Regulation; Battery Energy Storage System (BESS); Energy Management (EM).

I. INTRODUCTION

In recent years, there has been an increase in the demand for electrical energy, and because electrical energy generation relies mainly on traditional large power stations that rely on fossil fuels, this has led to environmental pollution and global warming. The search for sustainable sources of energy has become crucial for attaining sustainable development and protecting the environment in light of the environmental difficulties facing our world. This resulted in the creation of a brand-new form of electricity generation known as Distributed Generation (DG). Distributed generation can make use of both unconventional renewable energy generation methods like sunlight, wind, water, etc., as well as small-scale conventional power generation methods like micro and gas turbines [1][2].

In general, distributed generation, storage, and load clusters used to enhance the dependability and quality of local power systems and supply are referred to as Microgrids. Microgrids can be AC, DC, or DC-AC hybrid Microgrid [3]. However, DC Microgrid is preferred since it has less complicated control, doesn't have problems with grid synchronization, has harmonics and reactive power, and has lower conversion losses [4][5]. Applications for standalone or isolated Microgrids include homes, mobile phone towers, electric vehicles, marine ships, spaceships, submarines, etc.[6]. Naturally, Microgrid need algorithms to control operation as well as to manage power in order to provide loads with the necessary power at the appropriate voltage level in various operating conditions, as well as to manage and transfer power between sources and loads [7][8][9].

In this research, photovoltaic cells were used as a source of renewable energy. As a promising and long-lasting source of clean energy, photovoltaic (PV) panels have gained popularity. A photovoltaic cell is an item that uses solar radiation to produce electricity [10]. Sun PV array power output is influenced by the sun irradiation value [11][12]. As a result, the location and climate affect how much electrical energy can be produced by solar panels [13][14]. Without specialized technology, solar panels won't be able to produce at their full capacity. Maximum power point tracking(MPPT), also referred to as MPPT, is a method used to maximize the amount of electricity that solar panels can produce [15][16][17]. Incremental Conductance (InCond) and Observation and perturbation (P&O) are two popular traditional MPPT approaches that can be used [18][19][20]. These methods are usually used because of their affordability, simplicity of use, and easiness. However, each of these methods has shortcomings. PV systems wobble around MPP due to operating point variations that occur when they reach MPPT [21][22]. Likewise, P&O is also unable to apply MPP in systems with frequent changes in the environment because of slower convergence. A (InCond) MPPT technique has a extra complex algorithm than P&O because it can manage rapid changes in irradiance

and allows for variation in current over voltage; nevertheless, this approach has drawbacks, including vagueness in identifying step size and associated oscillations [23]. In this work, in order to obtain the maximum power, a method is utilized that depends on predictive Artificial Neural Networks (ANN), the MPPT based on Proportional and Integral controller (PI), and ANN (Hybrid ANN + PID). The PID was used to enhance the performance of ANN and eliminate its flaws, as it needs reliable data for training and testing, While the ANN algorithm tracks the maximum power point (MPP) by estimating the voltage at that point (reference voltage) using real-time data like temperature (T) and solar radiation (Irr), the PI controller looks for errors in the voltage difference between the measured and the reference voltage and makes the necessary adjustments to the process. However, the voltage generation by solar panels is not steady or constant, even using MPPT. It varies based on variations in sunlight and load [24]. This can cause problems for some devices or systems that require a consistent voltage input. Since the stability of the voltage profile is a vital and important requirement for the DC Microgrid [25]. In order to regulate voltage, lessen the effects of intermittent energy sources, and preserve the DC Microgrid power quality, energy storage technology and an appropriate power management plan must be employed [26][27]. A large amount of work has been done on voltage regulation on a Microgrid's DC bus such as in literature [28][29]. But, anytime there is an abrupt change in the inputs, control, or outputs (i.e., loads connected to the DC bus) voltage depressions and swells. In this work, we will try to reduce this problem and obtain a stable DC bus voltage level.

In this research, a power management algorithm consisting of several loops was proposed in order to obtain the maximum possible power from the PV panels by controlling the operation of the dc-dc boost converter. as well as to maintain DC bus voltage level and control the process of transferring excess power that generated by PV panels to the battery and storing it, this power will be used again if there is no generation or not enough power to supply for loads. this is done by controlling the switches S1 and S2 of DC-DC bidirectional converter. Where the bi-directional converter helps with effective control of the battery energy storage system (BESS), and This help to maintain the amount of power supplied even under heavy loads [30][31]. Various power flow management strategies and control technologies have been detailed in published work [32][33][34][35].

In this article, a Microgrid system will be described, containing photovoltaic panels as the primary source and a battery energy storage system as the secondary energy source. The PV panels are connected to the DC bus via a boost converter, and the battery is connected to the DC bus via a bidirectional converter. This paper contributes to the use of a power tracking algorithm based on artificial neurons and integrated with a PID controller in order to obtain the maximum power from solar panels, and propose a power management algorithm is to manage the distribution of power in a Standalone Microgrid, also managing the charging and discharging of the battery, and maintaining the DC bus voltage level by controlling the power converters that connected in the DC Microgrid.

The structure of this document is as follows. The system is described and modeling in Section 2. The strategies of control and power management of DC Microgrid are presented in Section 3. Section 4 showcases System simulation and results under different operating conditions. A comparison between MPPT algorithms is made in Section 5. The paper's conclusion in Section 6.

II. SYSTEM DESCRIPTION

In order to achieve the contribution of this research, which is to propose a new algorithm for DC Microgrid energy management, as well as to use one of the modern methods to obtain the largest possible amount of energy from solar panels. A clear roadmap for performing simulations, obtaining results, and completing the DC Microgrid power management process has been drawn for this research. Fig. 1 shows the most important steps followed in this work.

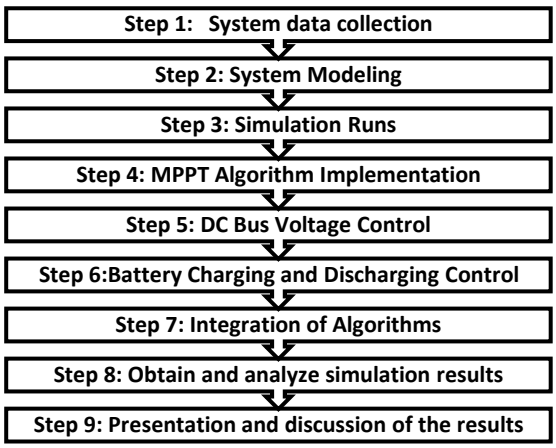

Fig. 1. Flow chart of research

Beginning, a DC Microgrid is illustrated, whose power sources consist of photovoltaic panels with a battery energy storage system, as in Fig. 2, to compensate for any shortage of power or to store the surplus of power produced. In addition to the photovoltaic array and the storage system, the system consists of electronic energy converters, where the photovoltaic panels are connected to the DC bus via a boost converter in order to raise the output voltage of the photovoltaic panels to the required level. The battery is connected to the DC bus using bi-directional DC-DC converters to control the process of charging and discharging the battery, and the loads are connected to the DC bus directly.

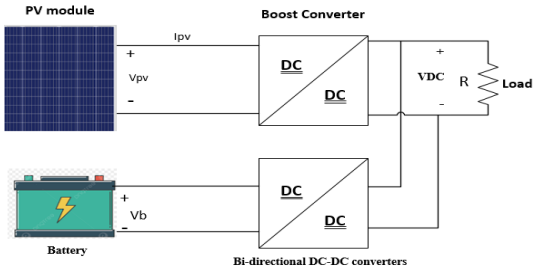

Fig. 2. Block diagram of the DC microgrid

A. Photovoltaic Cell Model

In general, a photovoltaic system consists of modules connected in series or parallel, each consisting of several photovoltaic cells [36]. The analogous circuit for solar cells is seen in Fig. 3, along with the equation connecting the circuit's current and voltage as [37][38].

$$I_L = I_{ph} - I_s \left(e^{\frac{q(V+IR_s)}{AKT}} - 1 \right) - \frac{V + I\,R_s}{R_{sh}} \quad (1)$$

Where D indicates a nonlinear diode, R_s is the series resistance, and Rsh indicates a parallel resistance. IPh indicates the photocurrent. T is the cell's absolute temperature (K), A indicates the $P-N$ junction ideality factor, Q indicates the coulomb constant, K indicates Boltzmann's constant, and I_s indicates the diode saturation current.

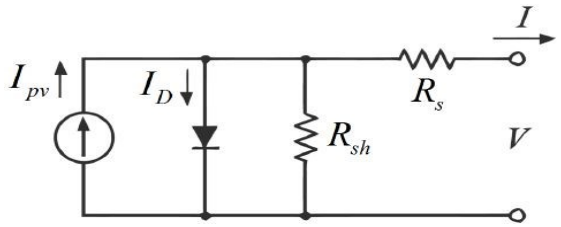

Fig. 3. The equivalent circuit of a solar cell

B. DC-DC Boost Converter Model

Power converters that boost voltage form their input source into their output are known as boost converters. Here, the input source is a solar panel's voltage. The circuit diagram for the boost power converter is shown in Fig. 4.

An unregulated DC voltage produced by clean energy can be raised to a higher voltage needed by loads by using a boost converter. The components of this circuit are load resistance (R), capacitance (C), and inductance (L). I and V denote, respectively, the voltage output at the capacitor's ends and the current passing through the inductor. To calculate the parameter values for a dc-dc boost converter, utilize equations (2)-(5) in [24]. An dc-dc boost converter has an output voltage that is greater than its input voltage, expressed as follows:

$$V_{dc} = \frac{V_{PV}}{1-D} \quad (2)$$

Where V_{pv} indicates the input voltage, D indicates the duty cycle, and V_{dc} indicates the output voltage. To achieve the process of raising the voltage in the boost, the value of D must be between zero and one. Calculating the output current is achievable by.

$$I_{dc} = I_{PV}\,(\,1-D\,) \quad (3)$$

In order for the converter to run in continuous current conduction mode, an inductance must be large enough such a way that the current flowing through the inductor IL is always continuous and never zero, as specified by:

$$L_1 \geq \frac{D(\,1-D\,)^2 R}{2f} \quad (4)$$

Where R indicates load resistance, L_1 indicates minimum inductance, and f indicates the booster converter's switching frequency.

The output voltage ripple is around 2%, as indicated in [39]. This ripple can be reduced by having a large enough capacitor on the output, after calculations were performed to find the amount of output capacitance and inputting capacitor that would provide the appropriate output voltage.

$$C \geq \frac{D}{\Delta\, Vdc\, fR} \quad (5)$$

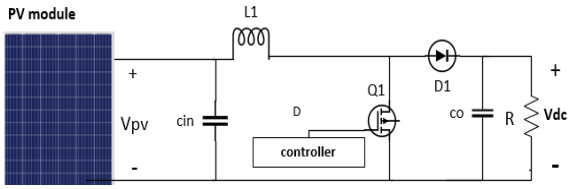

Fig. 4. The block structure for a boost converter

C. DC-DC Bidirectional Model

The DC-DC Bidirectional Converter is considered the primary link between the DC Microgrid and the autonomous BESS [16]. Its primary job is to give the Microgrid steady functioning and control. Typically, DC-DC converters, such as boost and buck converters, lack the ability to handle bidirectional power streams. This restriction results from the structure's diodes, which obstruct the flow of current in the opposite direction [40]. In general, a unidirectional DC-DC converter's architecture could be changed to make it bidirectional by replacing the diodes with a governable switch. Fig. 5 shows the design of the bi-directional Converter.

The work of the bi-directional converter has been explained. When does it work as a boost converter and when does it work as a buck converter in previous research [30][41].

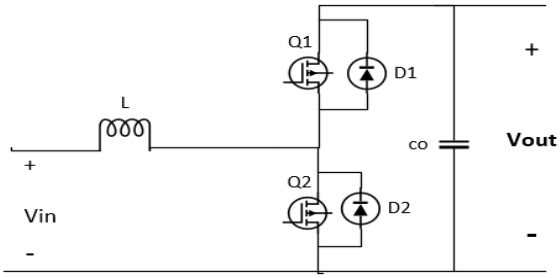

Fig. 5. The block structure for a Bi-directional converter

Choosing the inductor and the capacitor: The inductor's design affects how the converter operates overall. The size as well as the weight of a strong inductor which can be the biggest component in the entire converter are the main causes for concern. Selecting a low inductance value is required in order to reduce the weight and size of the inductor [42]. The critical inductance (LCR) value is the lowest inductance value that is anticipated to ensure that the converter operates in a continuous conduction mode (CCM). For the boost and buck converters, the critical inductance is (6) and (7).

$$L_{cr,boost} = \frac{T_S R_L}{2}(1 - D)^2 \quad (6)$$

$$L_{cr,buck} = \frac{(1 - D)T_S V_O}{2I_O} \quad (7)$$

Where (R_L) indicates the load resistance, (T_S) indicates the switching period, and (D) indicates the duty cycle in the steady state.

Furthermore, the ripple voltage of the capacitor can be used to determine the input and output capacitances.

$$C_{in} = \frac{\Delta I_L}{8\Delta V_{in}} T_S \quad (8)$$

$$C_{out} = \frac{V_O D}{\Delta V_O R_L} T_S \quad (9)$$

Where ΔI_L indicates the inductor ripple current and ΔV_o indicates the output ripple voltage.

D. BESS Model

In a DC Microgrid, the selection of battery power and storage system size is critical due to the nature of unstable generation from renewable energy sources [43]. Which ensures a constant supply of electricity even in times of low or intermittent solar energy production. By acting as a buffer zone, it increases the overall reliability and resilience of the grid by absorbing the excess energy generated by solar panels and releasing it when needed [44]. State of charge (SOC) and battery terminal voltage (VB) are two important factors for suggesting the battery status, these parameters are defined in [36][45]. There are several factors that affect battery capacity, such as the entire amount of energy required by loads from the battery bank, Deepest discharge possible, The highest possible power requirement, Voltage on the system and Current of charge and duration of recharge. In order to complete the mathematical design of the battery, we follow the equations in [12][44][46].

$$B_C = \frac{P_L \times Days\ of\ autonomy}{V_B \times DOD} \quad (10)$$

Where B_c indicates for the battery Capacity (Ah), PL indicates for the total power of the load, VB indicates for battery bus voltage, and DOD indicates for the Depth of Discharge.

The formula can be used to determine how many batteries must be connected in parallel in order for the system to reach the requisite Ah capacity.

$$B_P = \frac{B_C}{B_R} \quad (11)$$

Where B_P indicates for the number of Battery strings in parallel and BR indicates for the Capacity of selected battery.

The formula can be used to determine how many batteries must be connected in series to achieve the necessary system voltage:

$$B_S = \frac{V_B}{V_{bat}} \quad (12)$$

Where B_s indicates for the number of Battery connected in series and Vbat indicates for Selected Battery voltage.

III. CONTROL AND POWER MANAGEMENT OF DC MICROGRID

There are two steps in the control and management of energy process. Initially, an MPPT control is used to maximize the power extracted from the PV generator by means of the boost converter connected to it. Next, a DC bus voltage regulation is used to regulate the bidirectional converter connected to the batteries in order to govern the power between the load and PV.

A. DC-DC Boost Converter Control and MPPT Algorithm

In order to optimize the use of renewable energy produced by the photovoltaic array, the MPPT mode should be utilized for the boost converter. Fig. 6 Shows the components of the system in addition to explains the MPPT algorithm-based ANN and PID controller.

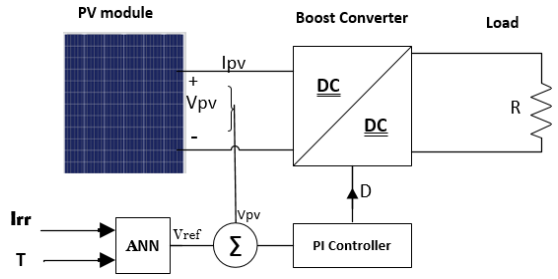

Fig. 6. The block structure for MMPT algorithm

This technique uses a PID controller along with artificial neural networks. ANN has many advantages, including offline training, fast tracking, and tolerance to nonlinearity [47][48][49]. As a result, numerous ANN-based PV MPPT methods have been developed recently. Prior research has demonstrated its effectiveness when compared to established conventional techniques [37][50]. Where ANN is composed of layers several layers Comprise input, hidden, and output layers that are modeled after real brain cells. The neurons are arranged into layers, and each layer has a large number of weighted connections with the other layers [51][52]. After training the maximum power point voltage of PV array is calculated, and compared to the measured voltage of the photovoltaic panels, and then, this difference is sent to a PI controller to obtain the appropriate duty ratio for PWM signal. PID gains are modified via a variety of techniques, including the Ziegler-Nichols approach and genetic algorithms [53][54].used the output signal to drive the switch to achieve maximum power tracking.

B. Bi-Directional DC-DC Converter Control and DC Bus Regulation

The energy storage system consists of a battery together with a bidirectional DC/DC converter and control system. Fig. 7 shows the bi-directional converter's control system, which is capable of controlling both directions of power flow. The converter functions as a buck circuit and charges the battery when S2 turns on and S1 turns off. Alternatively, the converter functions as a boost circuit and discharges the battery when S2 turns on and S1 turns off.

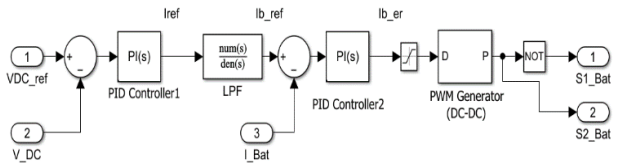

Fig. 7. Control of battery storage system

In this strategy, the bi-directional DC/DC converter is controlled via a dual-loop system, with the goal of achieving a high-quality, dynamic DC bus voltage. According to this scheme, the current of the battery reference, Ib_ref, is obtained by comparing the DC bus voltage VDC with its reference voltage Vref. This serves as the inner loop's input signal. Next, the difference between Ib_ref and the battery current, I_Bat, is sent into another PI controller to get the input signal for the PWM generator that causes S1 and S2 to turn on or off. Where maximum power can be extracted from the PV panel via the converter connected to the PV array. Then, DC bus voltage control via the bidirectional converter connected to the batteries is used in order to balance the power between the PV and the load. If any change in the DC bus voltage occurs, it may lead to problems in the regular operations of the system and may lead to their termination [55]. When in island mode, a battery absorbs extra energy produced by solar photovoltaic cells to keep the energy balance stable. The power management algorithm is represented in Fig. 8.

Power converters and power management algorithms work together to give the system the required control; the power management algorithms govern the operation of each system block and give the system intelligence [56]. It is noted in Fig. 9 the interconnection of the control algorithms in order to control the boost converter. If the SOC is higher than 98% the MPPT path will be closed. in other hand if SOC is less than 98% the MPPT path will be activated and battery will be charging.

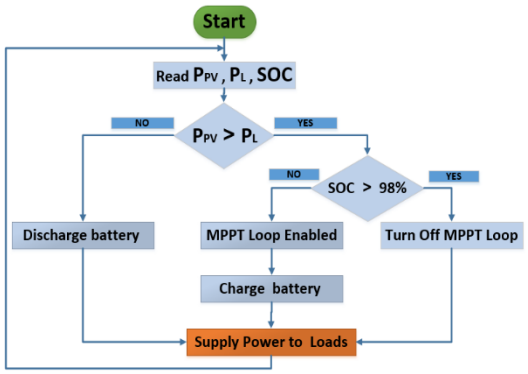

Fig. 8. Flowchart of power management algorithm

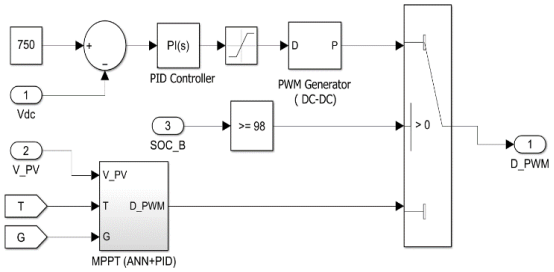

Fig. 9. Control of DC-DC boost converter

IV. Results of the Simulation and Discussion

In this part, the DC Microgrid will be simulated after completing the design calculations. The simulation will be carried out in the MATLAB environment under environmental conditions that simulate the climatic conditions surrounding the solar panels, where more than one scenario will be studied in terms of loading, temperature differences and solar radiation, and the results will be obtained, analyzed and discussed.

A. Simulation and Results

With MATLAB/Simulink software, the circuit diagram of a DC Microgrid was constructed following the design of system parameters, as shown in Table I. Fig. 10 shows the construction of A DC Microgrid. Two scenarios were simulated: (1) the DC Microgrid under constant load, and (2) the DC Microgrid under step-load changes. Both scenarios took into account a constant 25 °C temperature and solar irradiation ranging from 1000 to 500 W/m2. As seen in Fig. 11.

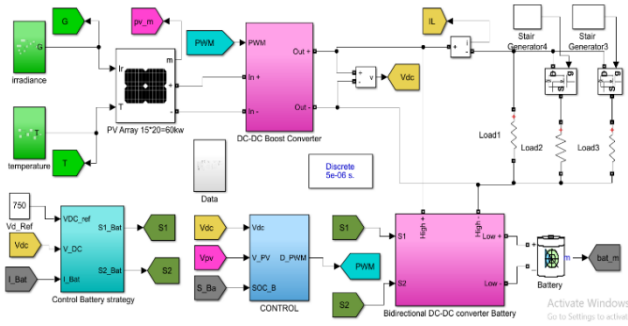

Fig. 10. The block structure for DC microgrid

TABLE I. Parameters for DC Microgrid

	Parameter	Value	Unit
PV SYSTEM	Maximum power(PMPP)	200.143	W
	Maximum power point voltage (VMPP)	26.3	V
	Open-circuit voltage (VOC)	32.9	V
	Maximum power point current (IMPP)	7.61	A
	Short circuit current (ISC)	8.21	A
	Number of series modules	15	-
	Number of parallel strings	20	-
Boost converter	Boost Inductor (L)	7.696	mH
	Output capacitor (Co)	1000	µF
	Input capacitor (Ci)	325	µF
Bidirectional converter	Inductor	0.8	mH
	Capacitor	100	µF
BESS	Type	Lithium-Ion	-
	Capacity	1000	Ah
	Voltage	690	V
	Initial SOC	70	%

Case 1: The DC Microgrid under constant load.

In this case, consider a constant temperature of 25 °C, and the solar irradiation value changes from 1000 to 750 W/m2 at the 4s, then decreases again to 500 W/m2 at the 8s. As shown in Fig. 11, The load value in this case is fixed at 45 kW.

When the simulation was carried out, the results appeared as follows. Fig. 12 shows the DC voltage level of the bus, Fig. 13 shows the power levels for each component in the DC Microgrid, and Fig. 14 shows the battery value results.

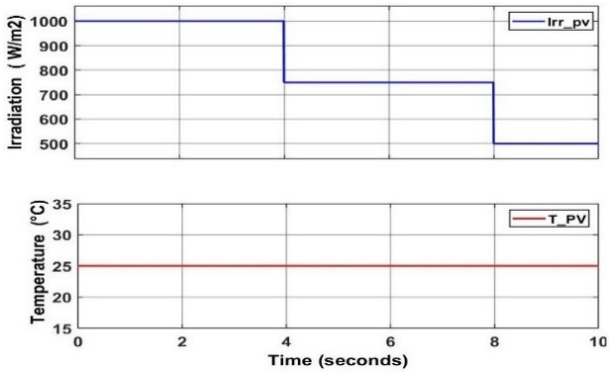

Fig. 11. Solar irradiance and temperature

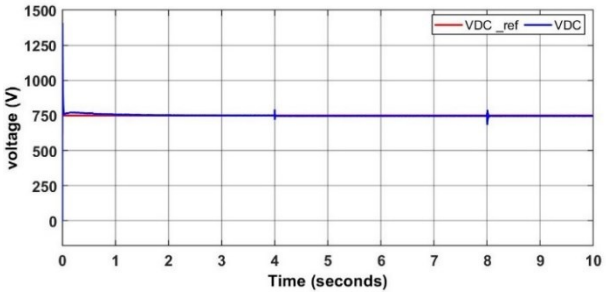

Fig. 12. VDC under constant load (case 1)

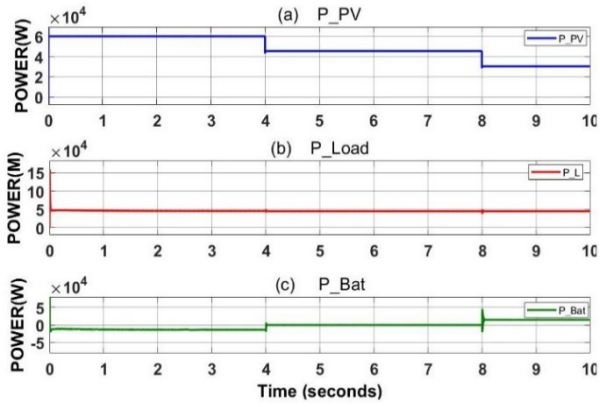

Fig. 13. Power curves (case 1) . (a) PV_Power, (b) Load power, (c) Battery Power

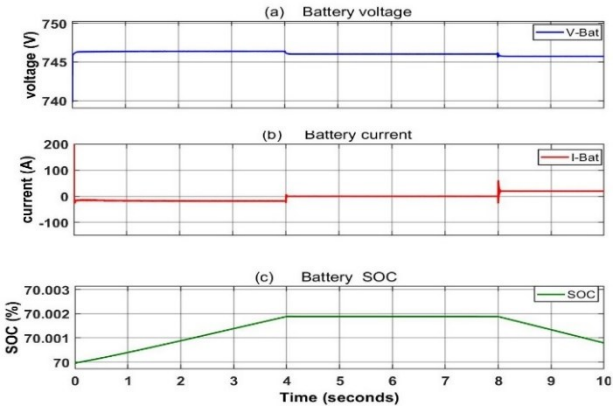

Fig. 14. The battery values results (case 1). (a) voltage, (b)current and (c) SOC

Case 2: The DC Microgrid under step-load changes.

In this case, the load is initially 30 kW from the start of operation until the 4s, then after that, the load rises to 45 kW, and at the 8s, the load rises to 60 kW, noting that the temperatures and solar radiation are identical to the first case, as shown in Fig. 11.

When the simulation was carried out, the results appeared as follows. Fig. 15 shows the DC voltage level of the bus, Fig. 16 shows the power levels for each component in the DC Microgrid, and Fig. 17 shows the battery value results.

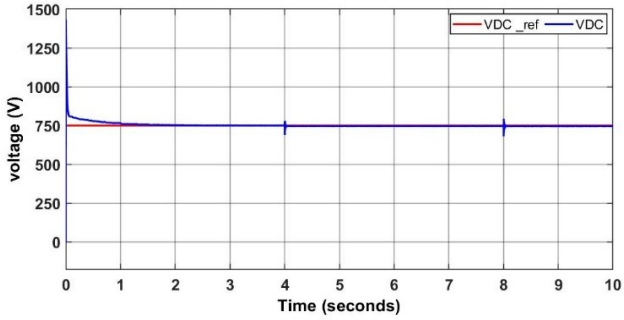

Fig. 15. VDC under change load (case 2)

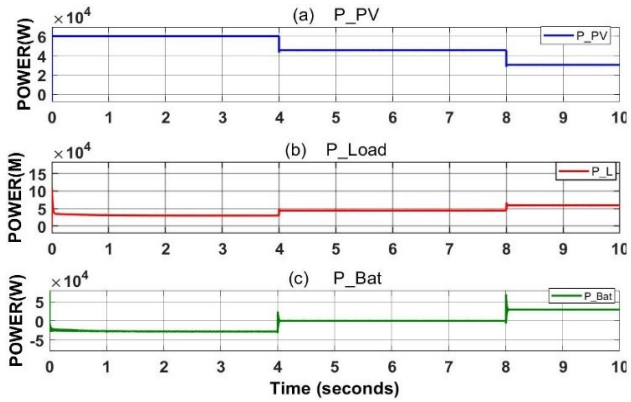

Fig. 16. Power curves (case 2). (a) PV_Power, (b) Load power, (c) Battery Power

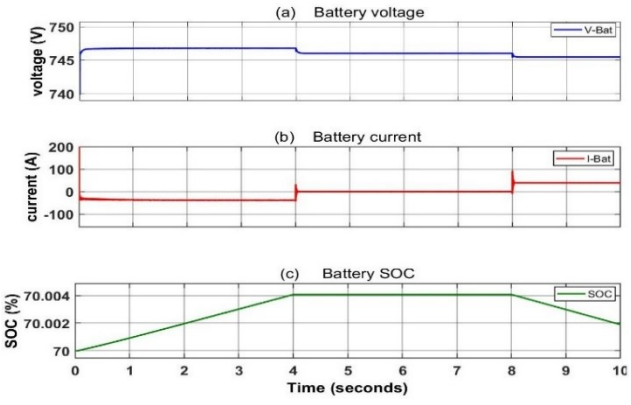

Fig. 17. The battery values results (case 2). (a) voltage, (b)current and (c) SOC

B. *Discussion*

In the first case, when performing the simulation where the load is constant, we notice in Fig. 12 that the DC bus voltage is almost identical to the required value of 750 volts,

even in the period when the generation is less than the load needs, the voltage difference is compensated for by the batteries through controlling on switches of bidirectional DC-DC Converter. with slight instantaneous fluctuations during the change in solar radiation.

Fig. 13 shows the power value of each component in the DC Microgrid. During the period from 0s to 4s, where the radiation was 1000 w/m, the power produced by the solar panels was greater than the value of the loads, the value of the power generated was 60 KW, while the load requirement was 45 KW, which means that 15 KW will be a surplus used to charge the battery via bidirectional DC-DC Converter, as shown in 13c. In the period between 4s and 8s, the decrease in solar radiation to 750 w/m led to a decrease in generation from the solar panels at 45 Kw, but the power generation value is completely identical to the load, and there is no surplus and no need for additional power, so there is neither charging nor discharging of the battery. As for the third period, which ranges from 8s to 10s, when the solar radiation drops to 500, the power produced becomes 30 kw, its insufficient to supply the loads. Here, the deficiency will be compensated by discharging the battery and using bidirectional DC-DC Converter. So, the battery value is 15 kw.

Fig. 18 shows an accurate picture of the power management process for case 1 in this system, as it contains a number of curves representing the power values for each part in the system. We notice a curve that shows the power produced by the solar panels, a curve that shows the required capacity of the load, and a curve that shows the power status of the battery in the charging state or the discharge is proportional to the amount of generation from the solar panels and the amount of power required for the load.

We also notice that this chart contains a curve representing a sum of the three power curve values. This sum represents the net power of the system, which should be zero according to the equation ($P_{NET} = P_{PV} + P_{Battery} - P_{Load}$).

Fig. 14 shows the battery values resulting from the simulation process for case 1. Fig. 14(a) shows the values of voltage, Fig. 14(b) shows the values of current, and Fig. 14(c) shows the state of charge of the battery for each of the three periods.

Note that in the first period, starting from 0s to 4s, Here the current value is less than zero and the curve of SOC represents the state of charge of the battery due to the presence of an excess of power generated by the solar panels. As for the second period, from 4s to 6s, the state of the battery is neither charging nor discharging and the current of battery equals zero, as the generated power is equivalent to the required load. In the third period, which begins at 8s, we notice a drop in the SOC curve and the current of battery more than zero, which means that there is a discharge of battery power to compensate for the decrease in production in order to feed the load with sufficient power.

In addition to that, note that the change in the battery voltage value is very small for the three time periods, so its value is considered stable.

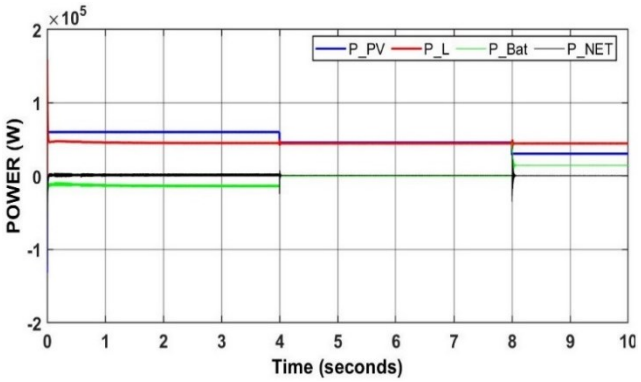

Fig. 18. Power management (case 1)

In case 2, when performing the simulation where the load is not constant, we notice in Fig. 15 that the DC bus voltage is almost identical to the required value of 750 volts, even in the period when the generation is less than the load needs, the voltage difference is compensated for by the batteries through controlling on switches of bidirectional DC-DC Converter. with slight instantaneous fluctuations during the change in solar radiation.

Fig. 16 shows the power value of each component in the DC Microgrid. During the period from 0 to 4, when the radiation was 1000 W/m, the power produced by the solar panels was greater than the load value, the value of the power generated was 60 KW, while the load requirement was 30 KW, which means that 30 KW will be a surplus used to charge the battery via bidirectional DC-DC Converter, as shown in 16c. In the period between 4s and 8s, the decrease in solar radiation to 750 watts/m led to a decrease in generation from solar panels, and despite the increase in the load to 45 kilowatts, the value of power generation is exactly identical to the load, and there is no surplus and no need for additional energy. So there is no charging or discharging of the battery. As for the third period, which ranges from 8 to 10 seconds, when the solar radiation decreases to 500 and the load increases to 60 kilowatts, the power produced becomes 30 kw, its insufficient to supply the loads. Here, the deficiency will be compensated by discharging the battery and using bidirectional DC-DC Converter. So, the battery value is 30 kw.

Fig. 19 shows an accurate picture of the power management process for case 2 in this system, as it contains a number of curves representing the power values for each part in the system. We notice a curve that shows the power produced by the solar panels, a curve that shows the required capacity of the load, and a curve that shows the power status of the battery in the charging state or the discharge is proportional to the amount of generation from the solar panels and the amount of power required for the load.

We also notice that this chart contains a curve representing a sum of the three power curve values. This sum represents the net power of the system, which should be zero according to the equation ($P_{NET} = P_{PV} + P_{Battery} - P_{Load}$).

Fig. 17 shows the battery values resulting from the simulation process for case 1. Fig. 17(a) shows the values of

voltage, Fig. 17(b) shows the values of current, and Fig. 17(c) shows the state of charge of the battery for each of the three periods.

Note that in the first period, starting from 0s to 4s, Here the current value is less than zero and the curve of SOC represents the state of charge of the battery due to the presence of an excess of power generated by the solar panels. As for the second period, from 4s to 6s, the state of the battery is neither charging nor discharging and the current of battery equals zero, as the generated power is equivalent to the required load. In the third period, which begins at 8s, we notice a drop in the SOC curve and the current of battery more than zero, which means that there is a discharge of battery power to compensate for the decrease in production in order to feed the load with sufficient power.

In addition to that, note that the change in the battery voltage value is very small for the three time periods, so its value is considered stable.

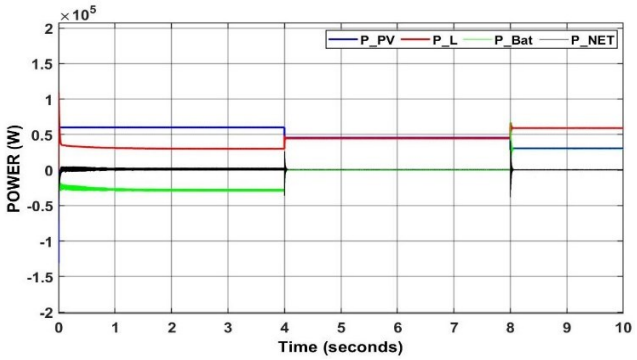

Fig. 19. Power management (case 2)

If we make a quick comparison of the two cases, the first case when the loads are constant and the second case when the load is variable, in Fig. 12, Fig. 15. Notice that the DC voltage curve for the first case responded faster than the second case, but in both cases the algorithm succeeded in maintaining the voltage level. Approximately to 750. and in Fig. 13, Fig. 16 notice that the PV voltage is not affected by the change in load, as it is identical in both cases and depends on the inputs (solar radiation and temperature). As for the battery power, it depends on the ratio of the generated power to what the load needs, but we notice that the power curve is more stable in case 1. As for Fig. 14, Fig. 17 which show the battery parameters for both cases, there is a lot of similarity between the two figures, and the only difference may be the state of battery charge in the second case, which was greater than the first case, depending on the power generation compared to the load requirements.

V. COMPARISON BETWEEN ANN + PID AND INCOND MPPT ALGORITHMS

There are many ways to calculate the maximum power of photovoltaic panels. To prove the efficiency of this method, it must be compared with one of the common methods. In this study, the ANN+PID method will be compared with the Incremental Conductance method (InCond). InCond method has been explained in several previous studies [57][58]. Many studies have also been conducted to compare different methods of MPPT [59][60][61]. In this work, the comparison is made under conditions similar to the first case that we studied in terms of temperature Constant at 25 °C and the load at 45 KW, and the difference is in solar radiation only the solar irradiance starts with a value of 700 W/m2, then rises at the 0.4s to 1000 W/m2, then at the 0.6s it decreases to 800 W/m2, then decreases again to 500 W/m2 at the 0.8s.

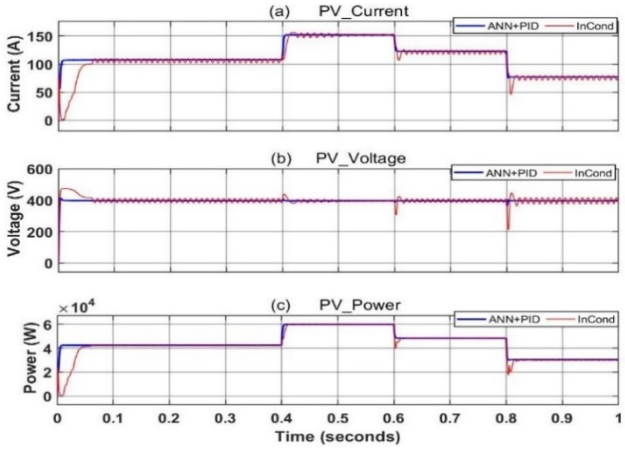

Fig. 20. Comparison results between MPPT algorithms (a) PV voltage (b) PV current (c) PV power

Fig. 20 shows the results obtained from the simulation process for comparing the voltage of a photovoltaic system using a traditional InCond and ANN+PID under a gradual change in radiation.

Fig. 20(a) shows the output current of the PV array used in this work. ANN+PID provided good results in terms of current oscillations and dynamic response compared to InCond. Fig. 20(c) shows the power curve, and the shape of the power curve is similar to the output current curve due to the fact that the current is directly proportional to solar radiation. While Fig. 20(b) shows the voltage curve, which is fairly constant with some disturbances at the moment when solar radiation changes. Whereas the voltages in the ANN + PID method were smoother and more stable than the InCond method, and if we look at all the curves in Fig. 12, we notice that all curves for ANN + PID were smoother compared to the InCond method, and the response was faster during variations in solar radiation, and Rise time for the ANN + PID method for all cases was less than the InCond method.

In addition to what has been explained, and in order for the comparison to be more comprehensive, we can analyze Fig. 20 more precisely, and we can also use some comparative indicators, as mentioned in [62]. Table II below shows the most important numerical comparisons between the two methods at 0.45s (Solar radiation = 1000W/m^{2}and temperature = 25 ◦C).

TABLE II. ANN+PID AND INCOND TECHNIQUE PERFORMANCE COMPARISON

Index	InCond	ANN+PID
Tracking power	59.49 Kw	60 Kw
Output current	146.7 A	151.9 A
Static efficiency MPP	99.07%	99.92%
Accuracy MPP	95.4%	99.85%

It is worth noting that when the simulation conditions were changed such that the change in temperature and load was also in addition to the change in solar radiation, the results were distorted and did not prove the superiority of the ANN +PID method in some parts of the curves obtained from the simulation. We also notice that at the moment of change in solar radiation or load, distortion and rise in the curves occur, and although they quickly return to stability, this distortion in ANN + PID is almost greater than it was in the traditional InCond method. This requires more and deeper study and more training of artificial neurons improve these results in the future. Also, to improve the power management algorithm, it is preferable to use the lowest limit of the State of charge (SOC_min) along with the maximum State of charge(SOC_max). After modification this algorithm will work to disconnect the battery from feeding the loads when the battery's power value drops to the lowest value. in order to avoid deep discharge and to preserve the life of the battery [63]. After making these modifications in terms of training and reprogramming neurons and modifying the energy management algorithm, this system can be further studied, tested, and implemented in clean energy applications that rely on solar energy, such as home applications or electric vehicles etc...

VI. CONCLUSION

In this study, a DC Microgrid system with loads, batteries, solar panels, and power converters for system control was created. The use of power tracking algorithms and power management algorithms to provide highly efficient power supplies to loads and keep the bus voltage within predetermined bounds is the primary objective. In this study, an algorithm based on artificial neurons was used and integrated with a PID controller in order to obtain the maximum power from solar panels by controlling the duty cycle of the boost converter. And it was compared with one of the traditional methods, and its reliability and efficiency were proven compared to the efficiency of the InCond algorithm. This Tracking algorithm was a great success, after simulation, the efficiency and accuracy of the ANN+PID algorithm reached 99.92% and 99.85%, respectively, while the efficiency and accuracy of the InCond method reached 95.4% and its efficiency reached 99.07% which provides the maximum power from photovoltaic panels. In addition, in order to simulate the energy management algorithm, two different scenarios were defined. The first was under the same climatic conditions in terms of constant temperature and variation in solar radiation. The first scenario depended on a constant load, while in the second scenario the load was variable. When running the simulation, the algorithm succeeded in both cases in maintaining the level of The DC bus voltage is 750 v, which is the value to be obtained. The algorithm also succeeded in managing the power in the two cases studied. When there was an excess in generation, the battery was charged, and when there was a deficiency in supplying power to the loads, it was compensated for by the battery and via controlling the switches of bidirectional Converter. These results enhance our understanding of complex energy management control systems. This work is an important step towards a more efficient and sustainable energy future by highlighting how future energy management algorithms can be developed to be better suited to real conditions, this highlights the importance of using neurons and artificial intelligence in obtaining the maximum power from solar panels, and thus their importance in making energy management algorithms. This contributes to the development of multiple applications such as home applications, electric vehicles, and other applications Important in our daily life.

REFERENCES

[1] T. Debela and A. Bhattacharya, "Design and analysis of a DC/AC microgrid with centralized battery energy storage system," in *IECON 2017-43rd Annual Conference of the IEEE Industrial Electronics Society*, pp. 8779–8784, 2017.

[2] O. A. Towoju and O. A. Oladele, "Electricity Generation from Hydro, Wind, Solar and the Environment," *Eng. Technol. J.*, vol. 39, no. 9, pp. 1392–1398, 2021.

[3] Z. Bahij. *DC Microgrid Modeling and Control in Islanded Mode*. Rochester Institute of Technology, 2021.

[4] D. E. Olivares *et al.*, "Trends in microgrid control," *IEEE Trans. Smart Grid*, vol. 5, no. 4, pp. 1905–1919, 2014.

[5] A. A. Abbooda, H. M. Habbib, and M. A. Zohdyc, "Investigation of Fault Analysis for Renewable Energy Microgrid," *Eng. Technol. J.*, vol. 41, no. 8, pp. 1118–1129, 2023.

[6] T. Thomas and M. K. Mishra, "Control Strategy for a PV-Wind based Standalone DC Microgrid with Hybrid Energy Storage System," *2019 IEEE 1st International Conference on Energy, Systems and Information Processing (ICESIP)*, pp. 1-6, 2019, doi: 10.1109/ICESIP46348.2019.8938310.

[7] A. K. Hado, B. S. Bashar, M. M. A. Zahra, R. Alayi, Y. Ebazadeh, and I. Suwarno, "Investigating and optimizing the operation of microgrids with intelligent algorithms," *J. Robot. Control*, vol. 3, no. 3, pp. 279–288, 2022.

[8] D. Murugesan, K. Jagatheesan, P. Shah, and R. Sekhar, "Optimization of Load Frequency Control Gain Parameters for Stochastic Microgrid Power System," *J. Robot. Control*, vol. 4, no. 5, pp. 726–742, 2023.

[9] J. Kumar, A. Agarwal, and V. Agarwal, "A review on overall control of DC microgrids," *J. energy storage*, vol. 21, pp. 113–138, 2019.

[10] R. Alayi, H. Harasii, and H. Pourderogar, "Modeling and optimization of photovoltaic cells with GA algorithm," *J. Robot. Control*, vol. 2, no. 1, pp. 35–41, 2021.

[11] M. Kumar, "Solar PV Based DC Microgrid under Partial Shading Condition with Battery-Part 2: Energy Management System," *2018 8th IEEE India International Conference on Power Electronics (IICPE)*, pp. 1-6, 2018, doi: 10.1109/IICPE.2018.8709437.

[12] A. Bakundukize, M. Twizerimana, D. Bernadette, B. J. Pierre, and N. Theoneste, "Design and Modelling of PV Power Plant for Rural Electrification in Kayonza, Rwanda," *Journal of Energy Research and Reviews*, pp. 31–55, 2021. doi: 10.9734/jenrr/2021/v7i430197.

[13] S. Rüstemli, F. Dincer, and M. Almalı, "'Research On Effects Of Environmental Factors On Photovoltaic Panels and Modeling With Matlab/Simulink," *Prz. Elektrotechniczny*, vol. 88, no. 2, pp. 63–66, 2012.

[14] O. Eseosa and N. I. Wariboko, "Proposing Utilization of Photovoltaic (PV) Source into Power Distribution Network Using University of Port Harcourt as a Case Study," *J. Robot. Control*, vol. 2, no. 4, pp. 274–282, 2021.

[15] W. Bai, "DC Microgrid optimized energy management and real-time control of power systems for grid-connected and off-grid operating modes," 2021.

[16] A. El-Shahat and S. Sumaiya, "DC-microgrid system design, control, and analysis," *Electron.*, vol. 8, no. 2, 2019, doi: 10.3390/electronics8020124.

[17] H. A. Hussein, A. J. Mahdi, and T. M. Abdul-Wahhab, "Design of a boost converter with mppt algorithm for a pv generator under extreme operating conditions," *Eng. Technol. J.*, vol. 39, no. 10, pp. 1473–1480, 2021.

[18] C. Li, Y. Chen, D. Zhou, J. Liu, and J. Zeng, "A high-performance

adaptive incremental conductance MPPT algorithm for photovoltaic systems," *Energies*, vol. 9, no. 4, p. 288, 2016.

[19] M. Abdel-Salam, M.-T. El-Mohandes, and M. Goda, "An improved perturb-and-observe based MPPT method for PV systems under varying irradiation levels," *Sol. Energy*, vol. 171, pp. 547–561, 2018.

[20] K. Dahmane, B. Bouachrine, M. Ajaamoum, B. Imodane, S. Mouslim, and M. Benydir, "Hybrid MPPT Control: P&O and Neural Network for Wind Energy Conversion System," *J. Robot. Control*, vol. 4, no. 1, pp. 1–11, 2023.

[21] S. K. Kollimalla and M. K. Mishra, "A novel adaptive P&O MPPT algorithm considering sudden changes in the irradiance," *IEEE Trans. Energy Convers.*, vol. 29, no. 3, pp. 602–610, 2014.

[22] M. E. Ahmad, A. H. Numan, and D. Y. Mahmood, "A comparative study of perturb and observe (P&O) and incremental conductance (INC) PV MPPT techniques at different radiation and temperature conditions," *Eng. Technol. J.*, vol. 40, no. 02, pp. 376–385, 2022.

[23] F. Liu, S. Duan, F. Liu, B. Liu, and Y. Kang, "A variable step size INC MPPT method for PV systems," *IEEE Trans. Ind. Electron.*, vol. 55, no. 7, pp. 2622–2628, 2008.

[24] M. I. Juma, C. J. Msigwa, and B. M. M. Mwinyiwiwa, "Solar Pv Based Maximum Power Point Tracking Embedded Voltage Regulation for Micro-Grid Application," vol. 6, no. 06, pp. 552–558, 2019.

[25] K. Gowtham, C. V Sivaramadurai, P. Hariprasath, and B. Indurani, "A Management of power flow for DC Microgrid with Solar and Wind Energy Sources," in *2018 International Conference on Computer Communication and Informatics (ICCCI)*, pp. 1–5, 2018.

[26] M. I. Juma, B. M. M. Mwinyiwiwa, C. J. Msigwa, and A. T. Mushi, "Design of a hybrid energy system with energy storage for standalone DC microgrid application," *Energies*, vol. 14, no. 18, 2021, doi: 10.3390/en14185994.

[27] P. Singh and J. S. Lather, "Accurate power-sharing, voltage regulation, and SOC regulation for LVDC microgrid with hybrid energy storage system using artificial neural network," *Int. J. Green Energy*, vol. 17, no. 12, pp. 756–769, 2020.

[28] M. Juma, C. Msigwa, and B. M. M. Mwinyiwiwa, "Solar PV based on maximum power point tracking embedded voltage regulation for micro-grid application," *Int. J. Innov. Res. Adv. Eng. IJIRAE*, vol. 6, pp. 552–558, 2019.

[29] S. Sahu, G. Panda, and S. P. Yadav, "Dynamic modelling and control of PMSG based stand-alone wind energy conversion system," in *2018 Recent Advances on Engineering, Technology and Computational Sciences (RAETCS)*, pp. 1–6, 2018.

[30] T. Satyanarayana and R. Dahiya, "Autonomous Battery Storage Energy System Control of PV-Wind Based DC Microgrid," *Int. J. Ambient Energy*, vol. 42, no. 8, pp. 888–894, 2021.

[31] D. S. Obaida, A. J. Mahdib, and M. H. Alkafajia, "A Modified Global Management Controller for a Grid-connected PV System with Battery under Various Power Balance Modes," *Eng. Technol. J.*, vol. 41, no. 2, pp. 294–308, 2023.

[32] S. Ali, Z. Zheng, M. Aillerie, J.-P. Sawicki, M.-C. Pera, and D. Hissel, "A review of DC Microgrid energy management systems dedicated to residential applications," *Energies*, vol. 14, no. 14, p. 4308, 2021.

[33] M. Ahmed, L. Meegahapola, A. Vahidnia, and M. Datta, "Stability and control aspects of microgrid Architectures–A comprehensive review," *IEEE access*, vol. 8, pp. 144730–144766, 2020.

[34] L. H. Pratomo, A. F. Wibisono, and S. Riyadi, "Design and Implementation of Double Loop Control Strategy in TPFW Voltage and Current Regulated Inverter for Photovoltaic Application," *J. Robot. Control*, vol. 3, no. 2, pp. 196–204, 2022.

[35] G. M. Alshabbani, M. K. Abd, M. Ilyas, and O. Bayat, "Management of Micro-grid with (SM) to Decrease Electricity Bills by Using (CAEST)," in *2020 International Conference on Electrical, Communication, and Computer Engineering (ICECCE)*, pp. 1–6, 2020.

[36] B. Liang *et al.*, "Simulation analysis of grid-connected AC/DC hybrid microgrid," in *2018 13th IEEE Conference on Industrial Electronics and Applications (ICIEA)*, pp. 969–974, 2018.

[37] S. D. Al-Majidi, M. F. Abbod, and H. S. Al-Raweshidy, "Design of an intelligent MPPT based on ANN using a real photovoltaic system data," in *2019 54th International Universities Power Engineering Conference (UPEC)*, pp. 1–6, 2019.

[38] R. B. Roy *et al.*, "A comparative performance analysis of ANN algorithms for MPPT energy harvesting in solar PV system," *IEEE Access*, vol. 9, pp. 102137–102152, 2021.

[39] M. M. Iqbal and K. Islam, "Design and simulation of a PV System with battery storage using bidirectional DC-DC converter using Matlab Simulink," *Int. J. Sci. Technol. Res.*, vol. 6, no. 7, pp. 403–410, 2017.

[40] S. Sumaiya, "Modeling, Designing and Analysis of a Standalone PV DC Microgrid System," 2018.

[41] S. Jadhav, N. Devdas, S. Nisar, and V. Bajpai, "Bidirectional DC-DC converter in solar PV system for battery charging application," in *2018 international conference on smart city and emerging technology (ICSCET)*, pp. 1–4, 2018.

[42] R. Teodorescu, M. Liserre, and P. Rodriguez. *Grid converters for photovoltaic and wind power systems*. John Wiley & Sons, 2011.

[43] C. Phurailatpam, R. Sangral, B. S. Rajpurohit, S. N. Singh, and F. G. Longatt, "Design and analysis of a dc microgrid with centralized battery energy storage system," in *2015 Annual IEEE India Conference (INDICON)*, pp. 1–6, 2015.

[44] A. N. H. Hamoodi and F. S. Abdulla, "Design and sizing of solar plant for Qayarah general Hospital and simulation with the PV-SOL program," *NTU J. Eng. Technol.*, vol. 1, no. 1, pp. 67–71, 2021.

[45] L. K. Amifia, "Direct Comparison Using Coulomb Counting and Open Circuit Voltage Method for the State of Health Li-Po Battery," *J. Robot. Control*, vol. 3, no. 4, pp. 455–463, 2022.

[46] M. Hailu Kebede, "Design of Standalone PV System for a Typical Modern Average Home in Shewa Robit Town-Ethiopia," *American Journal of Electrical and Electronic Engineering*, vol. 6, no. 2. pp. 72–76, 2018, doi: 10.12691/ajeee-6-2-4.

[47] C. G. Villegas-Mier, J. Rodriguez-Resendiz, J. M. Álvarez-Alvarado, H. Rodriguez-Resendiz, A. M. Herrera-Navarro, and O. Rodríguez-Abreo, "Artificial neural networks in MPPT algorithms for optimization of photovoltaic power systems: A review," *Micromachines*, vol. 12, no. 10, p. 1260, 2021.

[48] R. Divyasharon, R. N. Banu, and D. Devaraj, "Artificial neural network based MPPT with CUK converter topology for PV systems under varying climatic conditions," in *2019 IEEE International Conference on Intelligent Techniques in Control, Optimization and Signal Processing (INCOS)*, pp. 1–6, 2019.

[49] R. Çelikel and A. Gündoğdu, "ANN-based MPPT algorithm for photovoltaic systems," *Turkish J. Sci. Technol.*, vol. 15, no. 2, pp. 101–110, 2020.

[50] Y. E. A. Idrissi, K. Assalaou, L. Elmahni, and E. Aitiaz, "New improved MPPT based on artificial neural network and PI controller for photovoltaic applications," *Int. J. Power Electron. Drive Syst.*, vol. 13, no. 3, p. 1791, 2022.

[51] Z. Dzulfikri, N. Nuryanti, and Y. Erdani, "Design and implementation of artificial neural networks to predict wind directions on controlling yaw of wind turbine prototype," *J. Robot. Control*, vol. 1, no. 1, pp. 20–26, 2020.

[52] H. S. Dakheel, Z. B. Abdullah, N. S. Jasim, and S. W. Shneen, "Simulation model of ANN and PID controller for direct current servo motor by using Matlab/Simulink," *TELKOMNIKA Telecommunication Comput. Electron. Control.*, vol. 20, no. 4, pp. 922–932, 2022.

[53] M. M. Gani, M. S. Islam, and M. A. Ullah, "Optimal PID tuning for controlling the temperature of electric furnace by genetic algorithm," *SN Appl. Sci.*, vol. 1, pp. 1–8, 2019.

[54] N. Allu and A. Toding, "Tuning with Ziegler Nichols method for design PID controller at rotate speed DC motor," in *IOP Conference Series: Materials Science and Engineering*, vol. 846, no. 1, p. 12046, 2020.

[55] C. N. Bhende, S. Mishra, and S. G. Malla, "Permanent magnet synchronous generator-based standalone wind energy supply system," *IEEE Trans. Sustain. energy*, vol. 2, no. 4, pp. 361–373, 2011.

[56] I. Tank and S. Mali, "Renewable based DC microgrid with energy management system," in *2015 IEEE international conference on signal processing, informatics, communication and energy systems (SPICES)*, pp. 1–5, 2015.

[57] C. S. Rajan and M. Ebenezer, "Modeling operation and simulation of interconnected dc microgrids," in *2020 International Conference on Power, Instrumentation, Control and Computing (PICC)*, pp. 1–6, 2020.

[58] L. Assiya, D. Aziz, and H. Ahmed, "Comparative study of P&O and INC MPPT algorithms for DC-DC converter based PV system on MATLAB/SIMULINK," in *2020 IEEE 2nd international conference on electronics, control, optimization and computer science (ICECOCS)*, pp. 1–5, 2020.

[59] M. Sarvi and A. Azadian, "A comprehensive review and classified comparison of MPPT algorithms in PV systems," *Energy Syst.*, vol. 13, no. 2, pp. 281–320, 2022.

[60] S. Motahhir, A. El Hammoumi, and A. El Ghzizal, "The most used MPPT algorithms: Review and the suitable low-cost embedded board for each algorithm," *J. Clean. Prod.*, vol. 246, p. 118983, 2020.

[61] O. Diouri, A. Gaga, S. Senhaji, and M. O. Jamil, "Design and PIL Test of High Performance MPPT Controller Based on P&O-Backstepping Applied to DC-DC Converter," *J. Robot. Control*, vol. 3, no. 4, pp. 431–438, 2022.

[62] D. Ounnas, D. Guiza, Y. Soufi, and M. Maamri, "Design and hardware implementation of modified incremental conductance algorithm for photovoltaic system," *Adv. Electr. Electron. Eng.*, vol. 19, no. 2, pp. 100–111, 2021, doi: 10.15598/aeee.v19i2.3881.

[63] S. Adhikari, Z. Lei, W. Peng, and Y. Tang, "A battery/supercapacitor hybrid energy storage system for DC microgrids," in *2016 IEEE 8th International Power Electronics and Motion Control Conference (IPEMC-ECCE Asia)*, pp. 1747–1753, 2016.